Institute of Physics Publishing Journal of Physics: Conference Series **5** (2005) 162–174
doi:10.1088/1742-6596/5/1/014 International Workshop on Particle Multiplicity in Relativistic Heavy Ion Collisions

Statistical model description of particle multiplicities in heavy ion collisions

Krzysztof Redlich

Institute of Theoretical Physics University of Wroclaw,
PL-50204 Wroclaw, Poland

E-mail: redlich@rose.ift.uni.wroc.pl

Abstract. The application of statistical thermal models to a description of particles production in heavy ion collisions is discussed. A relation of the equation of state obtained form the phenomenological analysis of particle multiplicities in heavy ion collisions with a recent findings in Monte Carlo simulation of Lattice Gauge Theory at finite temperature and chemical potential is discussed. A connection of chemical freezeout with a critical condition in heavy ion collisions is indicated.

1. Introduction

The main objective of the experiments with ultrarelativistic heavy ion collisions is to study properties of strongly interacting medium at high energy density [1]. If such a medium is of thermal origin then some of its properties could be possibly studied in terms of statistical thermodynamics [2, 3]. However, in heavy ion collisions, an additional complication arise that strongly interacting medium produced in the initial state is not a static object but it undergoes expansion. A detailed analysis of experimental data at AGS, SPS and RHIC energies shows that such an expansion can be well described by an ideal hydrodynamics [4, 5]. This is particularly evident when considering dynamical observables like e.g. ecliptic or transverse flow. The total particle multiplicity, on the other hand, is only rather weekly influenced by the collective motion [6] and at freezeout can be well described as being originating from a static thermal fireball [2]. The thermodynamical properties of such fireball are in general characterized by the temperature T, the baryon chemical potential μ_B and the volume of the system. The temperature is the measure of thermal excitation, whereas μ_B describes the net baryonic density of QCD medium. These thermal parameters also determined densities of different particle species. The overall volume of the fireball is needed to describe the particle yields at fixed densities.

In this paper we summarized some recent results for multiplicities of different particle species obtained in heavy ion collisions in a very broad energy range from SIS, AGS, SPS up to RHIC. The results will be presented for central Au–Au or Pb–Pb collisions and compared with the predictions of thermal models.

One of the essential predictions of statistical QCD is deconfinement and chiral symmetry restoration. Thus, in the T–μ_B plane one expects a boundary line that separates the state where quarks and gluons are confined within hadrons and the chiral symmetry is spontaneously broken from quark–gluon plasma phase where color is deconfined and chiral symmetry is approximately restored. The position of such a boundary line is in general calculable within statistical QCD

on the lattice [7, 8, 9, 10]. On the other hand, the chemical freezeout conditions [2, 11] imposed empirical constraints on the position of the phase boundary line in (T–μ_B)–plane. In this paper we will discuss the relation between the chemical freezeout conditions obtained from thermal analysis of particle production in nucleus–nucleus collisions and recent lattice results at finite baryon density. In particular we show that when extrapolating present lattice results to chiral limit the critical conditions for deconfinement coincide approximately with chemical freezeout in heavy ion collisions in the energy range from SPS up to RHIC.

2. Thermodynamics of collision fireball

In a thermal model the basic quantity that is required to calculate thermal composition of particle yields measured in heavy ion collisions is the partition function $Z(T, V)$. In the grand canonical ensemble,

$$Z(T, V, \vec{\mu}_Q) = \mathrm{Tr}[e^{-\beta(H-\sum_i \mu_{Q_i} Q_i)}], \tag{1}$$

where H is the Hamiltonian of the system, Q_i are the conserved charges and μ_{Q_i} are the chemical potentials that guarantee that the charges Q_i are conserved on the average in the whole system. Finally $\beta = 1/T$ is the inverse temperature.

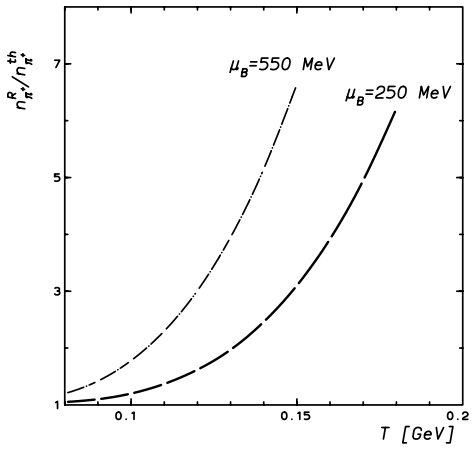

Figure 1. The ratio of the total density of positively charged pions that includes all resonance contributions to the density of thermal pions. The calculations are done in the hadron resonance gas model for μ_B =250, 550 MeV and for different temperatures.

The phenomenological partition function used to describe particle productions in heavy ion collisions was, following Hagedorn, constructed as non–interacting hadronic gas which is composed of all hadrons and resonances. In this approach the interactions between hadrons are included to the extent that the thermodynamics of an interacting system of elementary hadrons is effectively approximated by that of mixture of ideal gases of stable particles and resonances. The hadron resonance gas HRG–partition function 1 can be written then as a sum of partition functions $\ln Z_i$ of all hadrons and resonances

$$\ln Z(T, V, \vec{\mu}) = \sum_i \ln Z_i(T, V, \vec{\mu}), \tag{2}$$

where $\vec{\mu} = (\mu_B, \mu_S, \mu_Q)$ with the chemical potentials μ_i related to the baryon number, strangeness and electric charge, respectively. For particle i of strangeness S_i, baryon number

B_i, electric charge Q_i and spin–isospin degeneracy factor g_i, the fugacity

$$\lambda_i(T,\vec{\mu}) = \exp(\frac{B_i\mu_B + S_i\mu_S + Q_i\mu_Q}{T}) \tag{3}$$

and the single particle contribution

$$\ln Z_i(T,V,\vec{\mu}) = \frac{VTg_i}{2\pi^2}\sum_{k=1}^{\infty}\frac{(\pm 1)^{k+1}}{k^2}\lambda_i^k m_i^2 K_2(\frac{km_i}{T}), \tag{4}$$

where K_2 is the modified Bessel function and the upper sign is for bosons and the lower one for fermions. The first term in equation 4 corresponds to the Boltzmann approximation. The density of particle i is obtained from equation 4 as

$$n_i(T,\vec{\mu}) = \frac{\langle N_i\rangle}{V} = \frac{Tg_i}{2\pi^2}\sum_{k=1}^{\infty}\frac{(\pm 1)^{k+1}}{k}\lambda_i^k m_i^2 K_2(\frac{km_i}{T}). \tag{5}$$

The partition function 2 is sufficient to describe the equation of the system composed of hadrons and resonances being in thermal and chemical equilibrium. However, the equation 5 is still not sufficient to describe different particle yields in heavy ion collisions as it contains only a thermal particle component. In the phenomenological application of statistical model for particle production of particular importance is to account for resonance decays into lighter particles. The average number $\langle N_i\rangle$ of particle i in volume V and temperature T, that carries strangeness S_i, baryon number B_i, and electric charge Q_i, is obtained from

$$\langle N_i\rangle(T,\vec{\mu}) \;=\; \langle N_i\rangle^{th}(T,\vec{\mu}) + \sum\nolimits_j \Gamma_{j\to i}\langle N_j\rangle^{th,R}(T,\vec{\mu}), \tag{6}$$

where the first term describes the thermal average number of particles of species i and the second term describes overall resonance contributions to particle multiplicity of species i. This term is taken as a sum of all resonances that decay into particle i. The $\Gamma_{j\to i}$ is the corresponding decay branching ratio of $j \to i$. The corresponding multiplicities in equation 6 are obtained from equation 5. The importance of the resonance contribution to the total particle yield in equation 6 is illustrated in figure 1 as the ratio of total to thermal number of positively charged pions. From this figure it is clear that at high temperature (or density) the overall multiplicity of light hadrons is indeed dominated by resonance decays.

At lower temperature for $T < 100$ MeV, the widths of the resonances have to be included [12] in equation 5. This is because the number of light particles coming from the decay of resonances is increased by the finite resonance width. Thus, the approximation of the resonance width by delta function is not justified. For the Boltzmann statistics one replaces the partition function in equation 4 by:

$$\begin{aligned}\ln Z_i(T,V,\vec{\mu}) \;&=\; N\,\frac{Vd_R}{2\pi^2}\,T\,\exp[(B_R\mu_B + Q_R\mu_Q + S_R\mu_S)/T] \\ &\int_{s_{min}}^{s_{max}} ds\, s\, K_2(\sqrt{s}/T)\,\frac{1}{\pi}\,\frac{m_R\Gamma_R}{(s-m_R^2)^2 + m_R^2\Gamma_R^2},\end{aligned} \tag{7}$$

where s_{min} is chosen to be the threshold value for the resonance decay and $\sqrt{s_{max}} \sim m_R + 2\Gamma_R$. The normalization constant N is adjusted in such a way that the integral over the Breit-Wigner factor gives 1.

The statistical model, outlined above, was used [2, 13, 14, 15, 16] to describe particle yields in heavy ion collisions. The model was compared with all available experimental data obtained

in the energy range from AGS up to RHIC. Hadron multiplicities ranging from pions to omega baryons and their ratios were used to verify that there is a set of thermal parameters (T, μ_B) which simultaneously reproduces all measured yields. These two parameters together with the fireball volume[1] at chemical freezeout are sufficient to determine all particle yields. In heavy ion collisions the values of strange μ_S and charge μ_Q chemical potentials are fixed from the initial conditions. The strangeness neutrality and initial charge conservation determine the relation between μ_S, μ_Q with temperature and baryon chemical potential.

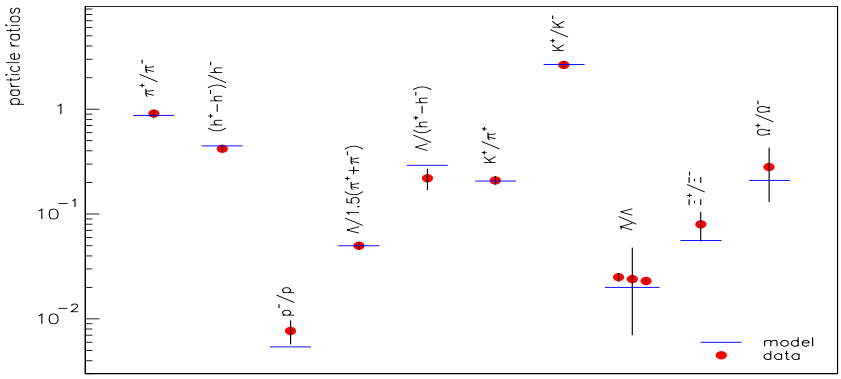

Figure 2. Comparison between thermal model predictions and experimental particle ratios for Pb–Pb collisions at 40 GeV/nucleon. The thermal model calculations are obtained with $T = 148$ MeV and $\mu_B = 400$ MeV [2].

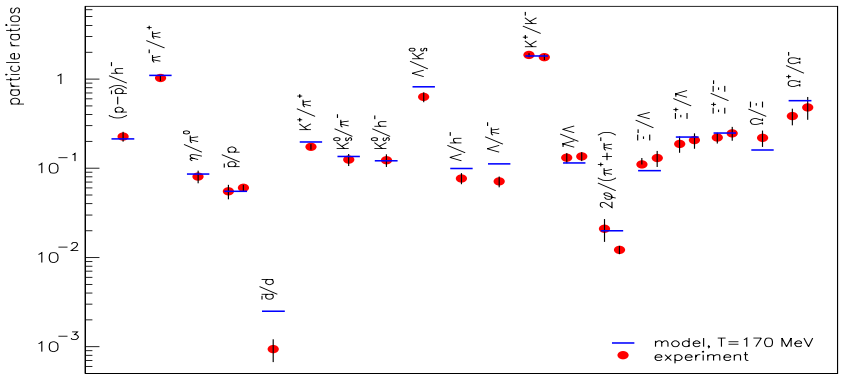

Figure 3. Comparison between thermal model predictions and experimental particle ratios for Pb–Pb collisions at 158 GeV/nucleon. The thermal model calculations are obtained with $T = 170$ MeV and $\mu_B = 255$ MeV [2].

Figures 2 and 3 show the comparison of thermal model with recent results of measured particle ratios for central Pb-Pb collisions at SPS energies (40 and 158 GeV/nucleon). An important issue in relating the model and data is whether to use data at mid-rapidity or data integrated over the full phase space. While it is clear that full 4π yields should be used at low beam energies, this is not appropriate any more as soon as fragmentation and central regions can be distinguished. In that case the aim is to identify a boost-invariant region near mid-rapidity and to choose a slice in rapidity within that region. For RHIC energies this implies that an appropriate choice, given

[1] The volume of the fireball can be possibly connected with HBT source size [17, 1].

the available data, is a rapidity interval of width $\Delta y = 1$ centered at midrapidity. The anti-proton/proton ratio stays essentially constant within that interval, but drops rather strongly for larger rapidities. Similar results are observed [18] for other ratios. Furthermore at RHIC, the rapidity distribution exhibits a boost-invariant plateau near mid-rapidity [19]. As has been demonstrated in references [6, 20], effects of hydrodynamic flow cancel out in particle ratios under such conditions. At SPS energies a boost-invariant plateau is not fully developed but stopping is not complete, either. In addition, the proton and anti-proton rapidity distributions differ rather drastically, especially near the fragmentation regions, implying that particle ratios depend on rapidity. Under those circumstances we show in figures 2 and 3 the model comparison with available data in a slice of ± 1 unit of rapidity centered at mid-rapidity. However, we have to be aware that choosing a restricted particle phase space could violate strangeness and charge conservation. In addition the resonances can be possibly distributed in larger rapidity windows. Thus, in application of statistical model to particle production in heavy ion collisions the values of thermal parameters contain some systematic errors. It is worth mentioning that at SPS energy the difference between chemical freezeout parameters extracted from experimental data at midrapidity and full phase space are consistent within statistical errors.

In comparison of the thermal model [2] with experimental data obtained in Pb-Pb collisions at 40 GeV/nucleon 11 particle ratios were included while the number was 24 at 158 GeV/nucleon as seen in figure 2 and 3. To get the best description of measured ratios the values for (T,μ_B) of (148±5, 400±10) and (170±5, 255±10) were obtained respectively with reduced χ^2 values of 1.1 and 2.0. Obviously the fits are quite good. A possible exception is the $\phi/(\pi^+ + \pi^-)$ ratio at top SPS energy, where there are conflicting data from NA49 and NA50. This is already discussed in detail in reference [15] and can be clarified within the recent measurements of ϕ yield by NA60 and CERES Collaborations. In addition, the yields of $\Lambda(1520)$ resonance do not follow statistical model systematics. Also the recent results of NA49 for kaon production show 20% deviations from the model. This will be disused in the next section.

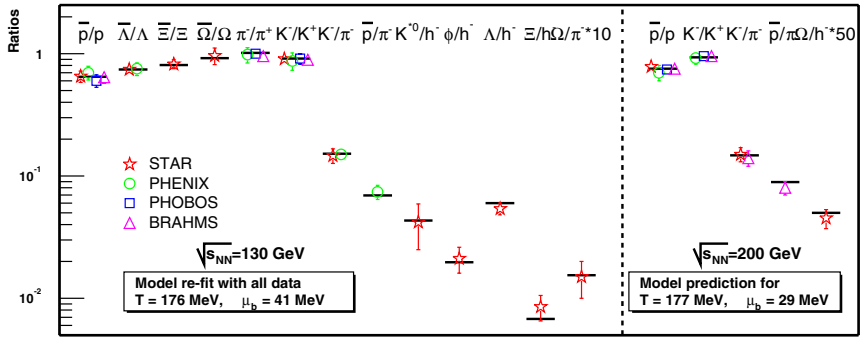

Figure 4. Comparison of the experimental data on different particle multiplicity ratios obtained at RHIC at $\sqrt{s}_{NN} = 130$ and 200 GeV with thermal model calculations. The thermal model analysis is from reference [13].

A comparison of thermal model with RHIC data in Au–Au collision at $\sqrt{s_{nn}} = 130$ and with part of the data obtained at $\sqrt{s_{nn}} = 200$ are shown in figure 4. A more complete thermal description of particle production at the top RHIC energy can be found in reference [21]. Figure 4 illustrates that thermal composition of particle yields is even more transparent than already seen at SPS energies. The goodness of the fit corresponds in this case to the value $\chi^2 < 1$. It is interesting to note that the yields of very rarely produced strange particles like Ω and even the yield of short lived resonance like $K^*(820)$ is well described by the model.

Recently, the STAR collaboration has provided [22] first data, with about 30 - 50 % accuracy, on the ratios involving ρ^0, $f^0(980)$, $\Lambda(1520)$ and K^{*0} resonances. The results were obtained for f_0/π^- and ρ^0/π^- in semi-central Au-Au collisions as well as for $\Lambda(1520)/\Lambda$ and K^{*0}/K ratios for different centralities. The yield of ρ^0 has been reconstructed for the first time in heavy ion collisions. From a perspective of thermal model the above ratios are interesting since resonances are essential degrees of freedom in the model. A large difference by a factor of four in the $\Lambda(1520)/\Lambda$ and a factor of two in K^{*0}/K ratios from p–p to central Au–Au collisions is unexpected. In a thermal model the temperature in p–p and Au–Au collisions is similar in the first approximation. In addition, the chemical potential dependence is week in both ratios. Thus, only a small variation with centrality of these observables could be expected. The $\Lambda(1520)/\Lambda \sim 5\%$ in thermal model agrees with the experimental result in peripheral Au–Au collisions but is obviously larger from that obtained in central collisions where $\Lambda(1520)/\Lambda \sim 2\%$. On the other hand in thermal model the $K^{*0}/K \simeq 32\%$ that differs from the mean experimental value of $\sim 40\%$ in p–p and $\sim 20\%$ in the most central Au–Au collisions.

The experimental results for $\Lambda(1520)/\Lambda$ and K^{*0}/K ratios required lower freezeout temperature than that obtained from the analysis of stable particle ratios. Actually the lower freezeout temperature is obtained in a thermal model proposed in reference [3] where the authors assumed that at chemical freezeout the thermal particle phase–space is out of equilibrium. Deviations from equilibrium were effectively parameterized by the fugacity parameters for different quark flavors. At RHIC the above off equilibrium model reproduces stable particle multiplicities as well and in addition due to lower freezeout temperature shows statistically better agreement with the measured $\Lambda(1520)/\Lambda$ and K^{*0}/K ratios in most central Au-Au collisions. Nevertheless, this model overestimate the experimental results too.

Interesting properties were also seen in STAR data for ρ^0 and f^0 yields. These mesons have been reconstructed in STAR via their decay channel in 2 charged pions. Comparing the preliminary results from STAR with statistical thermal model prediction reveals that the measured ratios exceed the calculated values by about a factor of 2. This is quite surprising, especially considering that a chemical freeze-out temperature of 177 MeV was used for the calculation, while one might expect these wide resonances to be formed near to thermal freeze-out, i.e. at a temperature of about 120 MeV. At this temperature, the equilibrium value for the ρ^0/π ratio is about $4 \cdot 10^{-4}$, while it is 0.11 at 177 MeV. Even with a chemical potential for pions being close to the pion mass and taking into account the apparent (downwards) mass shift of 60 - 70 MeV for the ρ^0 it seems difficult [23] to explain the experimentally observed value of about 0.18 [22]. The same is also seen in f^0/π^- ratio which in peripheral collisions reaches the value of $\sim 5\%$ whereas the equilibrium statistical model predicts this ratio to be smaller than $\sim 1\%$. The off equilibrium model [3] provides the values for f^0/π^- and ρ^0/π to be even lower than that in equilibrium approach, thus shows even stronger deviations from experimental results.

The actual data of STAR Collaboration for short lived resonances obtained in Au–Au collisions at 200 GeV seem to be inconsistent with thermal models. It is rather unlikely that any modification of this model e.g. through off equilibrium effects or modifications of particle masses could be capable of describing the yields of the above resonances and their centrality dependence. The observed deviations are most likely of dynamical origin and as such can not be handled in the effective thermal description. Until now however, there is no consistent quantitative understanding of the above data in terms of any dynamical or transport model [22]. We have to stress, however, that the actual failure of statistical approach in quantitative description of the yields of some short lived resonances does not invalidate the model nor the general concept of thermalization in heavy ion collisions. It should be rather considered as an indication that the assumption of chemical particle composition being preserved during the evolution from chemical towards kinetic freezeout does not necessarily hold for a short lived resonances. These particles are very sensitive to rescatterings [24] and collective medium effects [41] on the way from chemical

to thermal freezeout which could influence their measured multiplicities.

The equilibrium model discussed above was also applied to AGS data collected in reference [14]. The best fit of thermal parameters, obtained for Au–Au collisions at 14 AGeV yields T = 125 (+3-6) MeV and μ_B = 540 ±7 MeV.

Comparing the values of thermal parameters extracted from heavy ion data at different collision energies it is clear that with increasing energy there is a change of temperature and chemical potential at freezeout. However, at each collision energy there is only one set of thermal parameters that is required to reproduce experimental data for different particle multiplicity ratios.

3. From particle multiplicities to chemical freezeout conditions

Already the first analysis [11] of the chemical freezeout parameters obtained in central Pb–Pb or Au–Au collisions at top AGS, SPS and SIS energy have indicated that there is an interesting systematics in energy dependence of these parameters.

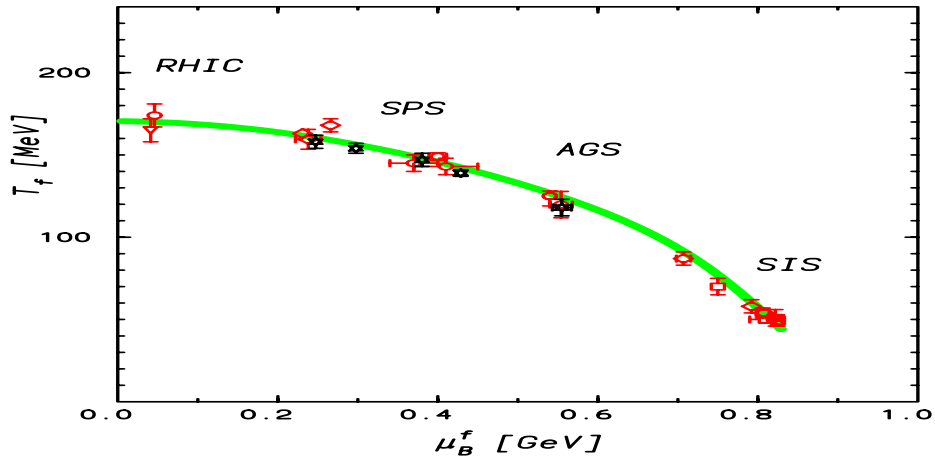

Figure 5. Chemical freezeout in heavy ion collisions. The full line represents the condition of fixed energy/particle $\simeq$ 1.0 GeV from reference [11]. The points are the average values of T and μ_B obtained from the analysis of particle yields in heavy ion collisions at the SIS, AGS, SPS and RHIC energy.

Figure 5 shows the compilation of all presently known freeze–out parameters that are required to reproduce the measured particle yields in central Au-Au or Pb–Pb collisions at SIS, AGS, SPS and RHIC energy. The GSI/SIS results have the lowest freeze–out temperature and the highest baryon chemical potential. As the beam energy increases, a clear shift towards higher T and lower μ_B occurs. There is a common feature to all these points, namely that the average energy $\langle E \rangle$ per average number of hadrons $\langle N \rangle$ is approximately 1 GeV. A chemical freeze–out in A–A collisions is thus reached [11] when the energy per particle $\langle E \rangle / \langle N \rangle$ drops below 1 GeV at all collision energies. The physical origin of the above freezeout condition requires dynamical justification. Recently, this point has been investigated in central Pb–Pb collisions at the SPS in terms of the Ultrarelativistic Quantum Molecular Dynamics model (UrQMD) [25]. A detailed study has shown that there is a clear correlation between the chemical break–up in terms of inelastic scattering rates and the rapid decrease in energy per particle. If $\langle E \rangle / \langle N \rangle$ approaches the value of 1 GeV the inelastic scattering rates drop substantially and the further evolution is due

to elastic and pseudo-elastic collisions that approximately preserved the chemical composition of the collision fireball. Following these UrQMD results one could consider the phenomenological chemical freeze–out of $\langle E\rangle/\langle N\rangle \simeq 1$ GeV as the condition of inelasticity in heavy ion collisions.

The chemical freeze–out in heavy ion collisions was also proposed to be determined [26] by the condition of fixed density of the total number of baryons plus antibaryons $F \equiv (n_B + n_{\bar{B}}) \simeq 0.12/fm^3$. Also recently this condition was formulated through fixed entropy density S per T^3 with $S/T^3 \simeq 7$ [27]. Within statistical uncertainties of phenomenological values of the freeze–out parameters the above conditions provide a good description of experimental data from the AGS up to RHIC energy. However, at the low SIS energy they both show deviations from presently established freezeout conditions. In Au–Au collisions at 1 AGeV the temperature $T \sim 50$ MeV and $\mu_B \sim 820$ MeV are required to get a consistent description of almost all data including kaons [12].[2] Taking the value of $F \sim 0.05/fm^3$ obtained at SIS energy and using the freezeout condition of $F_{SIS} = fixed$ leads eg. at RHIC to freezeout temperature of ∼150 MeV, the value which is lower than that obtained from the particle yield ratios as seen in figure 5). At $\mu_B = 0$ the $\langle E\rangle/\langle N\rangle$ condition converge to $T_f \simeq 170$ MeV. On the other hand at SIS the S/T^3 is calculated to be 12 instead of 7. Fixing $S/T^3 \sim 10 - 12$ and calculating the freezeout line one ends up with $T \sim 190 - 200$ MeV the value that exceeds the freezeout temperature at RHIC. The proposed chemical freezeout conditions of $F = fixed$ or $S/T^3 = fixed$ can not be apriori excluded. However, the presently known position of chemical freezeout at SIS energy favors the first phenomenological findings [11] that chemical freezeout appears at fixed energy/particle.

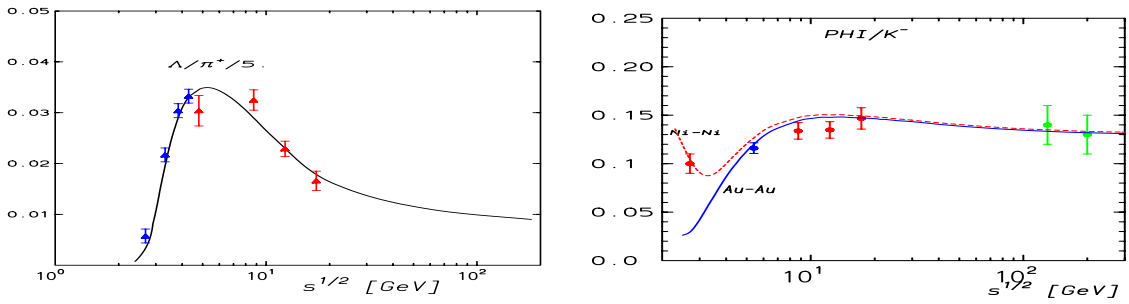

Figure 6. Left–hand figure: energy dependence of Λ/π^+ ratio. Right–hand figure: energy dependence of ϕ/K^- ratio. The lines are the hadron resonance gas model results obtained along unified freezeout line from figure 5. The points are the experimental data.

The phenomenological condition of chemical freezeout [11] turns out to be very powerful in predictions of particle production yields in heavy ion collisions. Applying the requirement of fixed $E/N \simeq 1$ GeV together with one experimental observable like e.g. the total number pions per participant allowed to establish the relation of freezeout temperature and chemical potential with collisions energy [29]. Consequently, predictions of thermal model for different particle excitation functions and other observables were established [29]. In figure 6 an example of such predictions is illustrated for Λ/π^+ [29] and ϕ/K ratios. The thermal model has predicted a rather sharp peak in Λ/π^+ ratio which is in good agreement with recent NA49 data. Also the surprising result of very flat dependence of the ϕ/K ratio between AGS and RHIC was recently confirmed by the data. On the other hand in the thermal model the K^+/π^+ ratio should exhibit a steep rise at low energies and subsequent flattening off with a mild maximum at $\sqrt{s} \simeq 10$GeV.

[2] Strangeness description at SIS energy required, however the canonical formulation of the conservation laws [12].

The recent results of NA49 Collaboration shows a rather sharp peak in K^+/π^+ ratio which can not be explained by the thermal model [28].

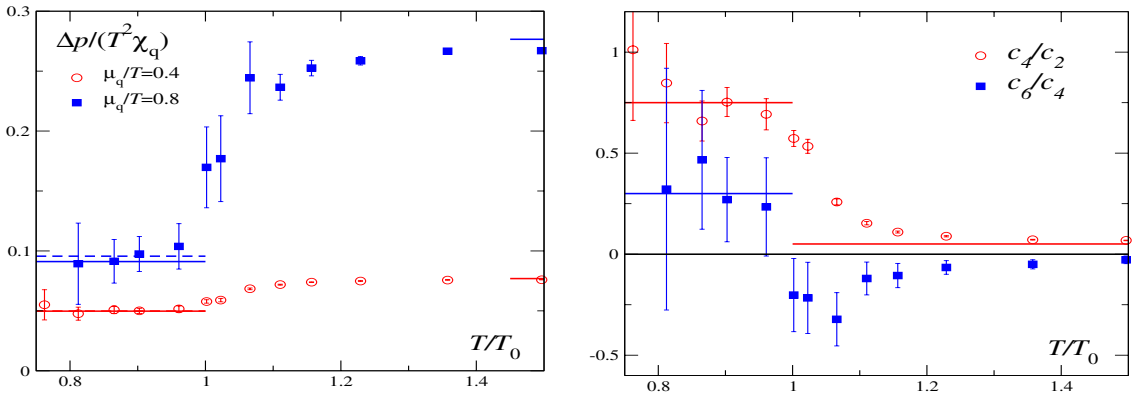

Figure 7. Left–hand figure: temperature dependence of $\Delta P/(\chi_q T^2)$ ratio for two different values of μ_q/T. The 2–flavor lattice results (points) are from [36, 38, 39]. The lines are the hadron resonance gas model values with (broken–line) and without (full–line) the Taylor expansion of $\cosh(\mu_B/T)$ [34, 38, 39]. The right–hand side shows the temperature dependence of the ratios of the second, fourth and sixth order coefficients in the Taylor expansion of thermodynamic pressure. The lines are the hadron resonance gas model results [34, 38, 39].

From the analysis of the energy dependence of freezeout parameters along the line of $E/N \simeq 1$GeV the position of chemical freezeout in Au–Au collisions at 40 and 80 GeV/nucleon, had been found [30] a few years before the data were taken. A detailed analysis of recent results of NA49 Collaborations shows that these predictions are in excellent agreement with the values obtained [31] from a direct fit of the model to experimental data . This shows that the thermal model has a predictive power to describe a bulk properties of different particle multiplicities and their energy dependence.

4. From chemical to critical conditions in heavy ion collisions

At SPS and RHIC the freeze-out parameters, the temperature T_f and the energy density ϵ_f, predicted by the presently used thermal model of hadron resonance gas, agree well [2, 32, 33, 34] with the values of the corresponding parameters required for deconfinement in LGT calculations [35, 36]. The above quantitative agreement of freeze-out and critical parameters suggests that at SPS and RHIC the chemical freeze-out appears in the near vicinity of the phase boundary [37]. If this is indeed the case, then the phenomenological statistical operator of hadron resonance gas should also provide, consistent with LGT, a description of QCD thermodynamics in confined, hadronic phase of QCD [32, 33, 38, 39]. The basic qualitative properties of the partition function 2 resulting from its T and μ_B dependence are indeed present in the recent lattice results obtained in two flavor QCD at the finite chemical potential. In addition with the hadron resonance gas partition function one can also describe [32] the quark mass and the number of flavor dependence of the lattice critical temperature at $\mu_B = 0$ and the position of the phase boundary in the (T, μ_B)–plane at small μ_B [34].

The net baryonic pressure $\Delta P = P(T, \mu_B) - P(T, \mu_B = 0)$ has been recently obtained [36] on the lattice in two flavor QCD as the Taylor series in μ_q/T

$$\frac{\Delta p(T, \mu_q)}{T^4} \simeq \sum_{n=1}^{n=3} c_{2n}(T) \left(\frac{\mu_q}{T}\right)^{2n} \tag{8}$$

up to $O(\mu_q^6)$ order from which the baryon density n_B and the baryon number susceptibility χ_q are obtained as the first and second order derivatives with respect to μ_q, respectively

$$\begin{aligned} \frac{n_q}{T^3} &= \frac{\partial\, \Delta P(T,\mu_q)/T^4}{\partial\, \mu_q/T} \simeq 2\, c_2(T) \left(\frac{\mu_q}{T}\right) + 4\, c_4(T) \left(\frac{\mu_q}{T}\right)^3 \quad + 6\, c_6(T) \left(\frac{\mu_q}{T}\right)^5 \\ \frac{\chi_q}{T^2} &= \frac{\partial^2\, \Delta p(T,\mu_q)/T^4}{\partial\, (\mu_q/T)^2} \simeq 2\, c_2(T) + 12\, c_4(T) \left(\frac{\mu_q}{T}\right)^2 + 30\, c_6(T) \left(\frac{\mu_q}{T}\right)^4 . \end{aligned} \tag{9}$$

The coefficients $c_i(T)$ in the Taylor expansion in equations 8 and 9 were calculated through the Monte–Carlo simulations of 2–flavor QCD [36].

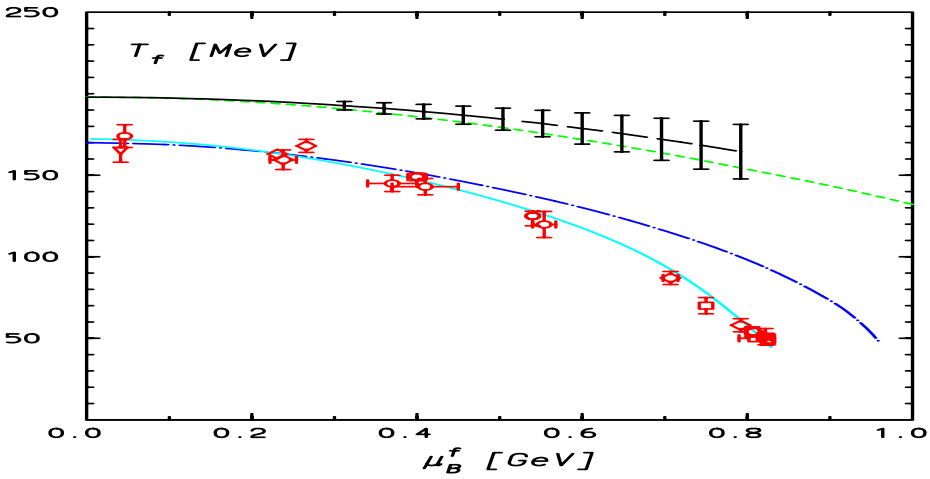

Figure 8. Lattice results [7, 36] on the phase boundary curve (line with errors) together with phenomenological freeze-out values of T and μ_B (points) obtained from the analysis of particle production in heavy ion collisions [2]. Short-dashed and dashed–dotted lines are the statistical model results [34] obtained under the condition of fixed $\epsilon \simeq 0.6$ GeV$/fm^3$ with $m_\pi \simeq 0.77$ GeV and $m_\pi \simeq 0.14$ GeV respectively. Also shown (full–line) is the phenomenological freeze-out curve of fixed energy/particle$\simeq$ 1GeV from [11].

The lattice results shown in equations 8-9 restricted to the confined phase of QCD can be directly compared with the predictions of the hadron resonance gas model. From equation 2 it is clear that in the Boltzmann approximation the hadron resonance gas provides the factorization of T and (μ/T) dependence of the net baryonic pressure

$$\frac{\Delta P}{T^4} \simeq F(T)(\cosh(\frac{\mu_B}{T} - 1) \qquad \text{with} \qquad F(T) \simeq \sum_i (\frac{m}{T})^2 K_2(\frac{m}{T}) \tag{10}$$

as well as the baryonic density and its fluctuations. Consequently, in the resonance gas model any ratios of n_q, χ_q and ΔP calculated at fixed quark chemical potential $(\mu_q/T) = fixed$, should be independent from temperature [32, 33, 38]. In figure 7–left we show as an example the ratio of $\Delta P/\Delta(\chi_q T^2)$ for two different values of μ_q/T as function of T. It is clear from figure 7–left that for $T < T_c$ the factorization predicted by hadron resonance gas model in equation 10 is also seen in LGT results.

The (μ_q/T)–dependence in the HRG–model is described by the (cosh)–function. Thus, performing the Taylor expansion of the pressure 10 in (μ_q/T) one gets the predictions on the values of the Taylor coefficients c_i in equation 8 from the phenomenological hadron resonance gas model

$$c_2(T) = \frac{9}{2}F(T)\ ,\ c_4 = \frac{81}{4!}F(T)\ ,\ c_6 = \frac{3^6}{6!}F(T). \tag{11}$$

Figure 7–right shows the ratios c_4/c_2 and c_6/c_4 obtained on the lattice in 2–flavour QCD and the corresponding results of the HRG–model from equation 11. The temperature dependence of the Taylor coefficients in equation 11 is controlled by a common function for all c_i. Thus, in HRG–model, the ratios of different c_i are independent of T. The lattice results for $T < T_c$ are, within statistical errors, consistent with this prediction. The values of c_6/c_4 and c_4/c_2 obtained recently on the lattice [36, 38, 39] are also seen in figure 7–right to coincide with HRG–model. At temperature $T \simeq T_c$, however, the lattice results deviate from the resonance gas values. This is to be expected as at the critical temperature, deconfinement releases the color degrees of freedom[3] which are obviously not there in the statistical operator of the hadron resonance gas. The partition function 2 is not sensitive to the phase transition thus, could be at most applicable below deconfinement.

The pressure calculated on the lattice increases abruptly when approaching deconfinement transition from the hadronic side [36, 38]. If the phenomenological statistical operator of hadron resonance gas is of physical significance then this increase could be due to the resonance formation. Indeed, a detailed comparison of the model with the lattice results has shown that the copious production of resonances provides a remarkable good description of temperature dependence of baryonic pressure and other observables [32, 33, 38, 39]. This indicates that phenomenological partition function of hadron resonance gas is a good approximation of QCD partition function in the confined phase.

The recent lattice results on QCD thermodynamics show that at vanishing μ deconfinement occurs at similar values of the energy density independently from the number of quark flavors and the quark mass [35]. Thus, the condition of fixed energy density could be considered as the criterium for deconfinement. This feature can also be seen at finite but small μ. Figure 8 shows recent lattice results on the position of the phase boundary line in 2–flavor QCD obtained within the Taylor approximation and with the pion mass $m_\pi \simeq 770$ MeV. The line of fixed energy density $\epsilon \simeq 0.6$ GeV$/fm^3$ with ϵ calculated in the HRG–model with the modified mass spectrum is seen to coincide with lattice results. Decreasing the pion mass to its physical value and including a complete set of resonances expected in (2+1)–flavor QCD results in the shift of the position of the phase boundary line towards a phenomenological freeze-out condition of fixed energy/particle$\simeq$ 1GeV. The splitting of freeze-out and phase boundary line appears most likely when the ratio of meson/baryon multiplicities reaches the unity [34].

The dashed–dotted line in figure 8 could be a physical boundary line separating the hadronic from the quark–gluon plasma phase. However, in the baryon dominating medium one expects a very efficient meson baryon scattering [41]. Consequently, the particle dispersion relations and spectral functions can be modified in a medium. Thus, it is not clear if the extrapolation of the dashed–dotted line in figure 8 towards larger $\mu_B > 500$MeV is adequate where the yields ratio (meson/baryon)< 1.

5. Summary

We have discussed some aspects of application of the statistical thermal model to the description of particle production in heavy ion collisions in a very broad energy range from SIS up RHIC. We

[3] These color degrees of freedom could be also possibly described as resonance bound states [40].

have shown that the hadron resonance gas partition function provides a satisfactory description of the bulk properties of the experimental data. The unified freezeout condition of fixed energy/particle being equal to 1 GeV turns out to be successful in predictions of particle excitation functions and freezeout parameters for different energies.

At present, there are, however, experimental findings which do not coincide with the statistical model predictions. The most serious deviations are seen on the level of short lived resonances measured at RHIC energy. In addition a sharp peak in the K^+/π^+ excitation function at SPS, obtained by the NA49 Collaboration, is not reproduced by the model. These deviations could be of dynamical origin and, at the moment, can not be handled within the statistical model approach.

We have shown that the phenomenological partition function of hadron resonance gas used in heavy ion phenomenology is also quite successful in describing recent LGT results on thermodynamics in confined phase at finite temperature and chemical potential. This indicates that the hadron resonance gas partition function is a good approximation of QCD thermodynamics in the hadronic phase. Applying the above partition function together with the condition of a fixed energy density we have discussed a possible position of the QCD critical curve in the temperature–chemical potential plane. As it turns out at SPS and RHIC the chemical freezeout appears close to deconfinement. However, at lower collision energies there is a splitting of critical and freezeout curve that, most likely, appears when the system passes from mesonic to baryonic dominating medium.

Acknowledgments
Stimulating discussions with R. Fini, B. Ghidini, E. Quercigh and K. Safarik, are kindly acknowledged. This work was supported by the KBN under grant 2P03 (06925).

References

[1] Satz H 2004 *Preprint* hep-ph/0405051
Gyulassy M and McLerran L 2004 *Preprint* nucl-th/0405013
[2] For recent review see e.g.: Braun-Munzinger P, Redlich K and Stachel K *Quark Gluon Plasma 3* (Edts. Hwa R and Wang X N) (*Preprint* nucl-th/0304013)
Andronic A and Braun-Munzinger P 2004 *Preprint* hep-ph/0402291
[3] Letessier J and Rafelski J 2002 *Cambridge Monogr. Part. Phys. Nucl. Cosmol.* **18** 1 and references therein
[4] Heinz U 2004 *Preprint* nucl-th/0407067
[5] Shuryak E 2004 *Prog. Part. Nucl. Phys.* **53** 273
[6] Cleymans J 2002 *J. Phys.* G **28** 1575
[7] Allton C R, Ejiri S, Hands S J, Kaczmarek O, Karsch, Laermann E, Schmidt C and Scorzato L 2002 *Phys. Rev.* D **66** 074507
[8] Fodor Z and Katz S D 2002 *Phys. Lett.* B **534** 87
[9] D'Elia M and Maria–Paola Lombardo 2003 *Phys. Rev.* D **67** 014505
[10] Petreczky P *Preprint* hep-lat/0409139
[11] Cleymans J and Redlich K 1998 *Phys. Rev. Lett.* **81** 5284
[12] Cleymans J and Redlich K 1999 *Phys. Rev.* C **60** 054908
Cleymans J, Oeschler H and Redlich K 1999 *Phys. Rev.* C **59** 1663
Cleymans J, Oeschler H and Redlich K 2001 *Phys. Lett.* B **485** 27
[13] Braun-Munzinger P, Magestro D, Redlich K and Stachel J 2001 *Phys. Lett.* B **518** 41
Magestro D 2002 *J. Phys.* G **28** 1745
[14] Braun-Munzinger P, Stachel J, Wessels J P and Xu N 1995 *Phys. Lett.* B **344** 43
Braun-Munzinger P, Stachel J, Wessels J P and Xu N 1996 *Phys. Lett.* B **365** 1
[15] Braun-Munzinger P, Heppe I and Stachel J 1999 *Phys. Lett.* B **465** 15
[16] Becattini F, Cleymans J, Keranen A, Suhonen E and Redlich K 2001 *Phys. Rev.* C **64** 024901
[17] Agakichiev G *et al* (CERES/NA45 Collaboration) 2004 *Phys. Rev. Lett.* **92** 032301
[18] Ouerdane D *et al* (BRAHMS Collaboration) 2004 *J.Phys.* G **30** S1129
[19] Ullrich T 2003 *Nucl. Phys.* A **715** 399

[20] Cleymans J 1997 *3rd International Conference on Physics and Astrophysics of Quark Gluon Plasma (ICPAQGP 97), Jaipur, India*
[21] Xu N and Kaneta M 2002 *Nucl. Phys.* A **698** 306
Kaneta M and Xu N 2001 *J. Phys.* G **27** 589
Kaneta M and Xu N 2002 *Nucl. Phys.* A **698** 306
Broniowski W and Florkowski W 2001 *Phys. Rev. Lett.* **87** 272302
[22] Fachini P 2004 *J. Phys.* G **30** S735
[23] Broniowski W Florkowski W and Hiller B 2004 *Preprint* nucl-th/0403046
[24] Torrieri G and Rafelski J 2003 *Phys. Rev.* C **68** 034912
[25] Bleicher M and Aichelin J 2002 *Phys. Let.* B **530** 81
[26] Braun-Munzinger P and Stachel J 2002 *J. Phys.* G **28** 1971
[27] Tawfik A 2004 *Preprint* hep-ph/0410329
[28] Cleymans J, Oeschler H, Redlich K and Wheaton S 2004 *Preprint* hep-ph/0411187
[29] Braun-Munzinger P, Cleymans J, Oeschler H and Redlich K 2002 *Nucl. Phys.* A **697** 902
[30] Redlich K and Tounsi A 2002 *Eur. Phys. J.* C **24** 589
[31] Manninen J *et al* 2004 *Preprint* nucl-th/0405015
[32] Karsch F, Redlich K and Tawfik A 2003 *Eur. Phys. J.* C **29** 549
[33] Karsch F, Redlich K and Tawfik A 2003 *Phys. Lett.* B **571** 67
[34] Karsch F, Redlich K and Tawfik A 2004 *J. Phys.* G **30** S1271
[35] Karsch F, Laermann E and Peikert A 2001 *Nucl. Phys.* B **605** 579
Karsch F, Laermann E and Peikert A 2000 *Phys. Lett.* B **478** 447
Karsch F 2002 *Nucl. Phys.* A **698** 199c
[36] Allton C R, Ejiri S, Hands S J, Kaczmarek O, Karsch F, Laermann E and Schmidt C 2003 *Phys. Rev.* D **68** 014507
[37] Stachel J 1999 *Nucl. Phys.* A **654** 119c
[38] Ejiri S, Allton C R, Doring M, Hands S J, Kaczmarek O, Karsch F, Laermann E and Redlich K 2004 *Preprint* hep-lat/0409033
[39] Ejiri S, Allton C R, Doring M, Hands S J, Kaczmarek O, Karsch F, Laermann E and Redlich K 2004 *Preprint* hep-lat/0408046
[40] Shuryak E 2004 *Preprint* hep-ph/0405066 and references therein
[41] Weinhold W, Friman B and Nörenberg W 1998 *Phys. Lett.* B **433** 236
Post M, Leupold S and Mosel U 2003 *Preprint* nucl-th/0309085
Brown G E, Guo-Qiang Li, Rapp R, Rho M and Wambach J 1998 *Acta Phys. Polon.* B **29** 2309
Schuryak E and Brown G E 2004 *Nucl. Phys.* A **717** 322